Numerical Study of the Air Conditioning of a Room by a Two-phase Thermosyphon Loop Using Meteorological Data from Mamou (Guinea)

Abdoulaye Diallo [a,b*], Xavier Chesneau [a], Idrissa Diaby [b]
and Djanfar El-Maktoume [a,c]

[a] *Laboratoire de Modélisation Pluridisciplinaire et Simulations (LAMPS), Université de Perpignan Via Domitia, 52, Avenue Paul Alduy, 66860 Perpignan cedex, France.*
[b] *Laboratoire d'Enseignement et de Recherche en Energétique Appliquée (LEREA), Université Gamal Abdel Nasser de Conakry, BP 1147, Conakry, Guinée.*
[c] *Laboratoire Energétique de l'équipe d'Accueil Doctoral physique du Globe, de l'Energie et de l'Environnement (PGEE), Université d'Antanarivo, Madagascar.*

Authors' contributions

This work was carried out in collaboration among all authors. All authors read and approved the final manuscript.

Original Research Article

ABSTRACT

This paper presents a numerical study of the air-conditioning of a room by a two-phase thermosyphon loop using meteorological data from the Mamou region (Guinea). The room is composed of a rectangular roof and a passenger compartment in the form of a parallelepiped. In addition, the air-conditioning unit that operates with methanol is composed of an evaporator, a condenser, a riser and a downcomer. The heat transfer modelling governing the habitat model and the air conditioning loop is based on the nodal method. The coupling of the system is done by convective transfer between the internal air of the habitat and the surface of the evaporator. The equations are solved by the implicit finite difference method. Thus, this resolution made it possible to determine the influence of the parameters on the model. This work presents results of the habitat with and without the air-conditioning loop for typical days in March of Mamou. These results show that the use of the air conditioning loop can contribute to lowering the internal air temperature. The

_____

Corresponding author: E-mail: abdulahjaloh@gmail.com, abdoulaye-1.diallo@univ-perp.fr;

value of the maximum temperature of the indoor air of the habitat with the air conditioner is about 299 K while that of the air without air conditioner is about 303 K. The variation of parameters such as temperature, wall thickness, incident solar flux, air exchange rate and evaporator surface has a significant impact on the operation of the air conditioner and on the temperature of the conditioned room. A low wall thickness or a high air exchange rate contributes to the temperature increase in the room. For a wall thickness of 10 cm, 15 cm or 40 cm, the air temperatures are 301.5 K, 297 K and 296.9 K respectively. However, for a habitat without an air conditioner the temperature is 303 K when the wall thickness is 15 cm.

NOMENCLATURES

Symbols

C_p : Heat capacity by mass $(J/kg.K)$

DF   : Solar flux density $(W/m²)$

e   : Thickness (m)

G_p : Incident solar flux density $(W/m²)$

h_{xij} : Heat transfer coefficient (W/m^2K)

hc   : Convective heat transfer coefficient (W/m^2K)

hr   : Radiation heat transfer coefficient (W/m^2K)

h_{fg} : Latent heat of vaporization (J/kg)

L   : Length (m)

M   : Mass (kg)

$\dot{m}$: Mass flow rate (kg/s)

N   : Air change rate (h^{-1})

Nu   : Nusselt number

Pr   : Prandtl number

Ra   : Rayleigh number

S   : Surface (m^2)

T   : Temperature (K)

t   : Time (s)

U   : Flow velocity (m/s)

V   : Volume (m^3)

v   : Wind velocity (m/s)

w   : The mass fraction

Δx : Step of distance (m).

Greek Symbols

α_p : Coefficient of absorptivity ;

Φ_i : Heat source or sink $(W/m²)$

ϕ_{ra} : Air renewal $(W/m²)$

β_m : Mass expansion coefficient (K^{-1})

σ : Stefan-Boltzmann constant (Wm^2K^{-4})

ε : Emissivity

ρ : Density (kg/m^3)

λ : Thermal conductivity $(W/m.K)$

σ_f : Surface tension (N/m)

μ : Dynamic viscosity $(kg/m.s)$

Index

a   : Ambient

ai   : Indoor air of the room

cd   : Condenser

e   : Outdoor

evap   : Evaporator

f   : Fluid

l   : Liquid

M   : Materials considered

pe   : Exterior wall

pi   : Inside wall

s   : Saturation

v   : Steam

vs   : Saturating steam

1. INTRODUCTION

In recent years, the trend of increasing demand for air conditioning, especially in buildings, has been observed in many countries. However, even if the figures vary from one country to another, it is argued that on a global scale, about 40% of the total building energy is consumed for space heating and cooling applications in residential and commercial buildings [1]. In most regions of Guinea like Mamou, the urbanization rate is increasing every day. Moreover, there is not thermal and energy regulation in this sector. Most often these buildings are poorly oriented and are subject to climatic effects (sunshine, wind, etc.) which can be severe and difficult to control. In addition to these constraints, global warming and the heat island effect combined with poor building design [2] contribute greatly to the increase in internal temperatures of the premises and require the integration of an efficient air conditioning system without energy consumption. At the same time, in this country the majority of the population lives in inadequate and overcrowded houses, sometimes with or without electricity. The demand for electricity far exceeds the supply due to population growth and urbanization rate, thus causing malfunctioning of electrical installations. Moreover, only 18% of the national population has access to electricity,

which is among the lowest rates in the sub-region [3]. However, electricity is the main source of energy for the operation of active air conditioning systems [4]. Hence the need to develop passive cooling techniques that reduce the energy consumption of buildings, protect the environment and the ecosystem and provide a satisfactory level of comfort to cope with this crisis. Two-phase thermosyphon loop air conditioning is one of the technologies that can achieve significant energy savings and carbon emission reductions. This system is a self-contained device that works with a temperature difference. A two-phase air-conditioning loop is able to dissipate high thermal power with a very low quantity of fluid, which is interesting when the working fluid becomes expensive or environmentally damaging. In addition to these advantages, this thermosyphon system is less bulky, less expensive and its application as a passive cooling loop offers the advantage of operating without any mechanical pumps and without noise [5,6]. A diphase cooling loop is mainly composed of an evaporator which represents the hot source to dissipate heat contained in a room and a condenser which represents the cold source and which allows to liquefy the heat transfer fluid. These two components are connected by pipes: a steam pipe and a liquid pipe. In order to ensure the gravity operation of the loop, the condenser must be placed above the evaporator [7]. Several researchers have done experimental and numerical studies on the thermal performance, optimum filling ratio, heat transfer methods and operating conditions of the two-phase thermosiphon loop in recent years. Chehade, A. et al. [8], have modelled and experimentally investigated a thermosyphon loop for cooling a telecommunication cabinet. The test was done with different working fluids. The system is studied to define the optimal pipe diameters (liquid and vapour) and the effect of ambient temperature on the mass flow rate and pressure drop of the fluid. The results show that the best working fluid is the one that gives a lower loop response time and thermal resistance. Indeed, increasing the pipe diameters by 0.012 m and 0.014 m would be a key factor in improving the system efficiency. On the other hand, increasing the outdoor ambient temperature negatively affects the cooling performance by increasing the mass flow in the loop and decreasing the evaporator pressure drop. Their prototype does not require a pump for the circulation of the heat transfer fluid. The equipment housings are placed in the center of the cabinet with the heat

adjusted by of an autotransformer. Cao, H., et al. [9] focused through an experimental study and numerical simulation to investigate the height of the downcomer refrigerant. The results indicated that a high refrigerant column height would occupy part of the condenser space and reduce the performance of the two-phase thermosiphon loop. Zhang, P., et al. [10] did a modeling and experimentation of a two-phase thermosiphon loop in which the downcomer can be partially or completely filled with liquid. In their study, it is shown that when the temperature difference and the refrigerant charge are very low then the downcomer is partially filled with liquid and increasing these would increase and then decrease the heat transfer rate. Khodabandeh, R. et al. [11] observed instabilities of different nature which appeared at low or very high heat fluxes and worsen with large diameter of the evaporator pipes. Tong, Z. et al. [12] experimentally tested the effects of fill rate on the operating stability of a loop using R744 as the working fluid. It is found that, the optimal fill rate to achieve the loop's ability to transfer maximum heat is 100%. Under the fill rate higher or lower than this value, the ability of the loop to transfer heat will be decreased. In another study [13], these same authors experimented with a two-phase thermosyphon loop using R744 and R22 under different heat transfer rates from 1 to 4 kW. In this study the thermal performance and resistance for cooling a data center are examined. It is found that, R744 offers better cooling performance and that its thermal resistance is 22-25% lower than that of R22. In this paper, we evaluate through a numerical study the heat transfer in a room integrating a two-phase thermosiphon loop for a dry and humid tropical climate. To do this, we propose a mathematical model based on the nodal method that describes the operation of the air conditioning loop and the habitat. The modelling concerns the heat transfers of the room and the air conditioning loop composed of an evaporator, a condenser, a riser and a downcomer. Then, we will make the coupling between the habitat and the air conditioning unit in order to observe the impact of the air conditioner on the temperature profile of the internal air of the room. Thus, we observe in the time, the evolution of the various parameters in the air-conditioned room. Finally, we present the influence of some input parameters in order to evaluate their impact on the air conditioning system including the thermal comfort of the habitat taking into account the climatic conditions of the city of Mamou.

2. METHODOLOGY AND MATERIALS

2.1 Presentation of the Study Area

Mamou, the study area is located 270 km from the capital Conakry, in the south of the central massif of Fouta-Djallon between 10° 22.53' North latitude and 12° 5.48' West longitude. The prefecture of Mamou covers an area of 8674.32 km² with an altitude of 720 m in relation to the sea level. The urban commune is limited to the East by the rural communes of Soyah and Dounet, to the West by Konkouré, to the North by Boulliwel and Tolo and to the South by Konkouré and Soyah (Fig. 1.). The relief and altitude in Fouta are the essential factors of the climate. Like middle Guinea in general, Mamou has a tropical (or foutanian) climate, characterized by two alternating seasons, a dry season (November to April) and a rainy season (May to October). The harmattan is felt in the dry season and the hygrometric degree of the air easily falls below 45%. Rainfall is very abundant with an average annual rainfall of 2.087 mm. Average monthly temperatures range from 294 K to 301 K. The highest maximum temperatures values are observed in march and april with an average temperature that sometimes reaches 310 K while the lowest minimum temperatures of about 284 K on average are recorded in december. As for the winds, apart from the harmattan and the monsoon which are dominant on the ground, the mountain and valley breezes blow regularly. The relief of the urban commune is uneven, consisting of plateaus forming the beginning of the Fouta Djallon massif, which makes it difficult to move between the different districts. The vegetation of the commune is very favoured. It is essentially made up of bamboos, cheese trees, cailcédrat, baobab and others. In addition, there is a wide range of fruit trees: Mango, Avocado, Papaya, Citrus, etc. There are also classified forests in Tyéwel, Sérè, Koumi, Diarabaka and Tambassa.
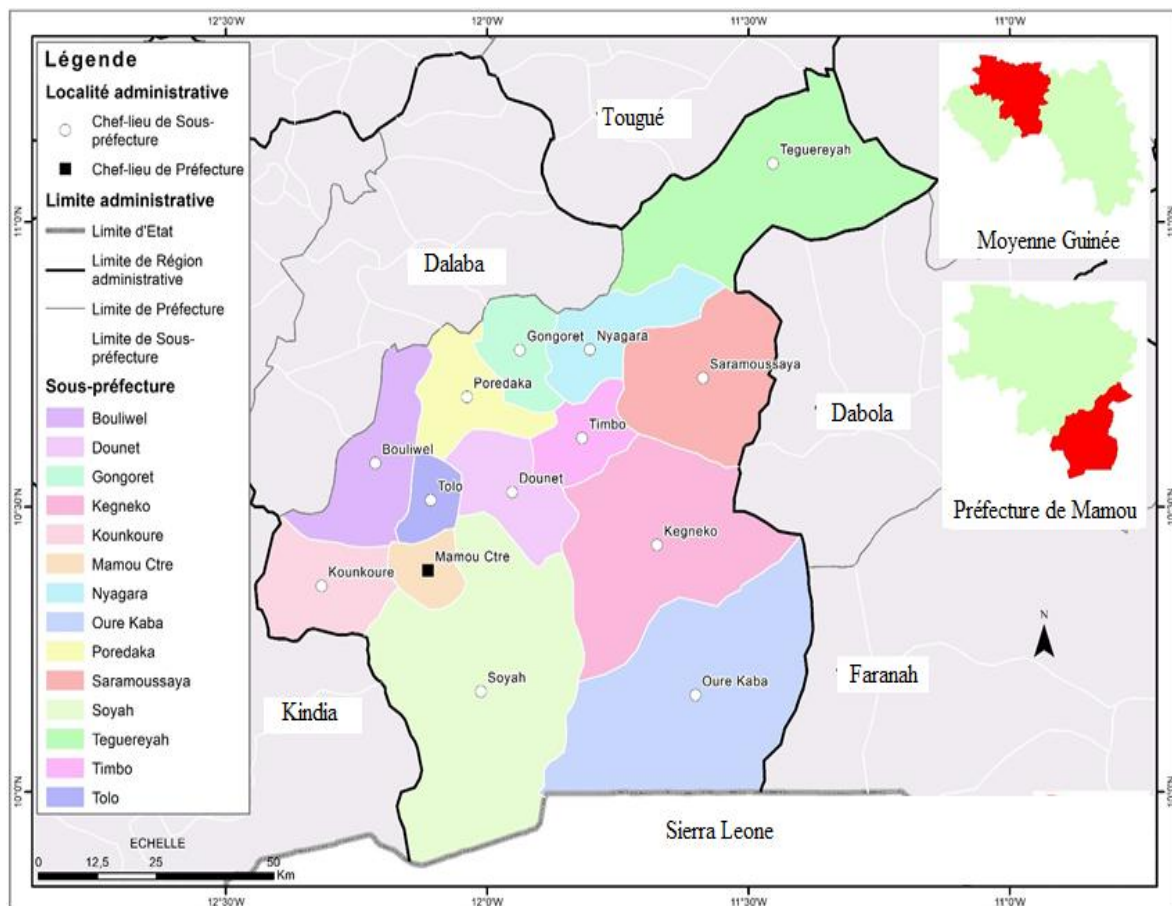

Fig. 1. Location of the study area.

2.2 Description of the Physical Model

The habitat model chosen for this study is a classic habitat typical of Guinea. It is composed of two parts: a roof and a living area. The roof is rectangular in shape, sloping towards the south make an angle of 30° to the horizontal and 0.5 m high. It is covered with galvanized steel sheets of a thickness of about 5 mm and a high thermal conductivity of about 50 W/m². The roof is separated from the passenger compartment by a false ceiling made of wooden counter plates which serve as insulation as shown on Fig. 2. The passenger compartment is a parallelepiped of the dimension 4x3x3 m with a surface of 12 m². The 15 cm thick wall, is built with clay bricks and concrete floor. The retained habitat model is equipped with an air conditioning loop consisting of an evaporator, a condenser, a riser and a downcomer. The evaporator is disposed in the room to be air-conditioned and the condenser outside the room (Fig. 2). The pipes are insulated in such a way that the heat loss of the heat transfer medium can be neglected. Copper is used as the material for the cooling loop. The thermo-physical properties of the materials for the habitat and the cooling loop are presented in Table 1.

2.3 Working Principle of the Model

The incident solar flux arrives on the roof and on the walls of the habitat. Due to the effect of the ambience and the incident solar flux, the various components of the habitat (the galvanized steel roof, wall, false ceiling, etc.) absorb heat during the day. This heat is transmitted to the indoor air of the habitat by conduction, by radiation and by convection. Thus, the indoor air temperature increases throughout the day. The different modes of heat transfer are illustrated on the Fig. 2. As for the air-conditioning loop, it operates with methanol as the heat transfer fluid. The refrigerant absorbs heat from the environment to be cooled and evaporates in the evaporator. The refrigerant vapour rises in the riser under the action of buoyancy forces generated by the differences in density of this fluid in the riser and the downcomer. It condenses in the condenser, releasing its latent heat of condensation. The condensate flows by gravity into the downcomer and returns in evaporator.

2.4 Mathematical Formulation

2.4.1 Assumptions

- Heat transfer is unidirectional;
- The temperature distribution on the inner and outer walls is uniform,
- The thermo-physical properties of materials are constant
- All the evaporated mass is condensed,
- One-dimensional fluid flow;
- Steam is an ideal gas;
- Boiling occurs at the evaporator;
- Condensation in the film occurs at the condenser.

2.4.2 Model equations

The heat transfer equations governing the model are based on the nodal method. Then, we establish a thermal balance based on the analogy between thermal and electrical transfers on each of the elements considered. Thus, we consider each node (i) an independent element from the others and we apply the law of conservation of energy. The heat transfer balance equation is written by [14,15]:

$$m_i Cp_i \left(\frac{\partial T_i}{\partial t} \right) = \alpha_i G_i + \sum_i h_{xij} S_i \left(T_j - T_i \right) + \Phi_i \tag{1}$$

Table 1. Thermo-physical properties of materials

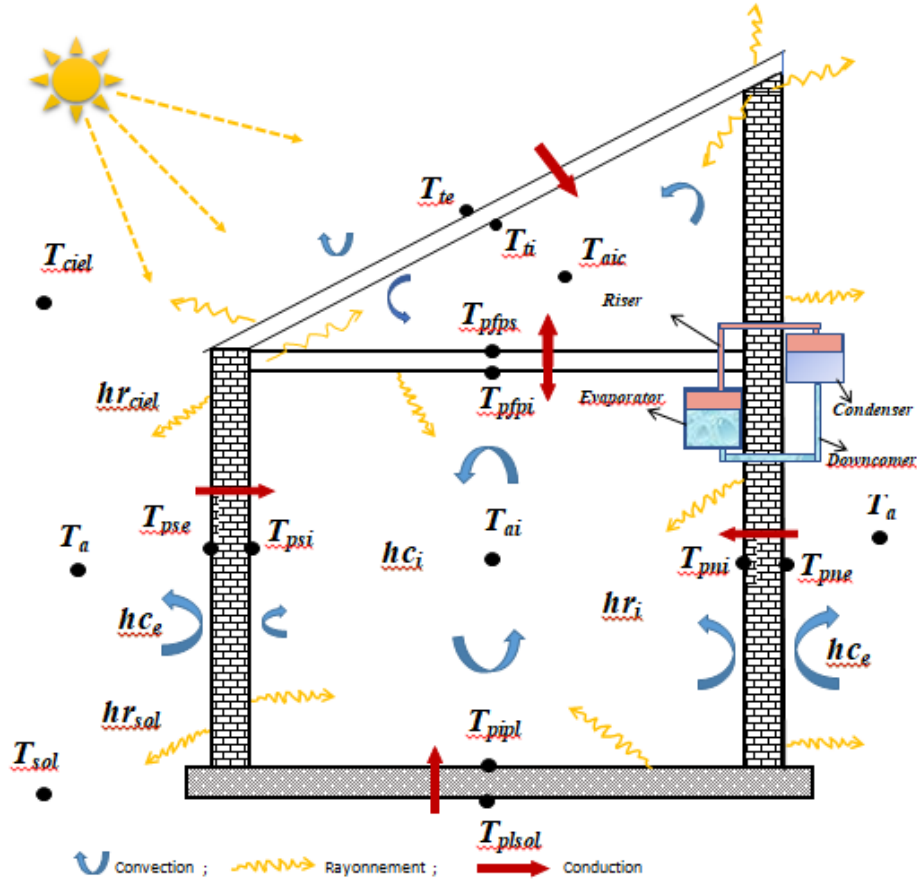| Materials	Density ρ (kg/m^3)	Heat capacity c_p $(J/kg.K)$	Thermal conductivity λ $(W/m.K)$
Habitat			
BTC	1850	1000	1.150
Galvanized steel sheets	7800	450	50
False ceiling in plywood	800	1600	0.24
Concrete	2300	100	0.8
The air conditioning loop			
Air	1.16	1006	0.0261
Copper	8900	380	380
Methanol (liquid)	786	4390	
Methanol (Steam)	0.218	1400	

Fig. 2. Different modes of heat transfer in the home

2.4.3 Heat transfer balance equation of the habitat

The heat transfer balance equation at the air level of the living area is written by :

$$\rho_{ai}V_{ai}c_{p,ai}\left(\frac{\partial T_{ai}}{\partial t}\right)=\sum_{j=1}hc_{j,pi}S_{j,pi}\left(T_j-T_{ai}\right)+hc_{evap}S_{evap}\left(T_{evap}-T_{ai}\right)+\phi_{ra}$$

(2)

With : $\phi_{ra}=0.34NV\left(T_a-T_{ai}\right)$

The heat transfer balance equation for all the external walls of the habitat is written as:

$$\frac{\rho_M V_M c_{p,M}}{S_{pe}}\left(\frac{\partial T_{pe}}{\partial t}\right)=\alpha_p G_p+\frac{\lambda_M}{e_M}\left(T_{pi}-T_{pe}\right)+hc_e\left(T_a-T_{pe}\right)+hr_{sky,pe}\left(T_{sky}-T_{pe}\right)+hr_{soil,pe}\left(T_{soil}-T_{pe}\right)$$

(3)

The heat transfer balance equation for all the internal walls of the habitat is written as:

$$\frac{\rho_M V_M c_{p,M}}{S_{pi}}\left(\frac{\partial T_{pi}}{\partial t}\right)=\frac{\lambda_M}{e_M}\left(T_{pe}-T_{pi}\right)+hc_i\left(T_{ai}-T_{pi}\right)+\sum_{j=1}hr_{j,pi}\left(T_j-T_{pi}\right)$$

(4)

2.4.4 Heat transfer balance equation of the air-conditioning loop

The heat transfer balance equation of the internal walls of the evaporator and the condenser is determined by:

$$\frac{mc_p}{S}\left(\frac{\partial T_{pi}}{\partial t}\right) = \frac{\lambda_M}{e_M}\left(T_{pe} - T_{pi}\right) + hc\left(T_f - T_{pi}\right)$$

(5)

Heat transfer balance equation at the external walls

- At the evaporator

$$\frac{mc_p}{S}\left(\frac{\partial T_{pe}}{\partial t}\right) = hc\left(T_a - T_{pe}\right) + \frac{\lambda_M}{e_M}\left(T_{pi} - T_{pe}\right)$$

(6)

- At the condenser

$$\frac{mc_p}{S}\left(\frac{\partial T_{pe}}{\partial t}\right) = \alpha_p G_p + hc\left(T_a - T_{pe}\right) + \frac{\lambda_M}{e_M}\left(T_{pi} - T_{pe}\right) + hr_{soil}\left(T_{soil} - T_{pe}\right) + hr_{sky}\left(T_{sky} - T_{pe}\right)$$

(7)

Heat transfer balance equation at the fluid level

- At the evaporator

$$m_f c_{pf}\left(\frac{\partial T_f}{\partial t}\right) = \sum_{j=1} hc_j S_j\left(T_{j,pi} - T_f\right) - \dot{m}\, h_{fg}$$

(8)

The flow rate is calculated by:
$$\dot{m} = S\beta_m\left[w_{vs}\left(T_s\right) - w_v\left(T\right)\right]$$

(9)

- At the condenser

$$m_f c_{pf}\left(\frac{\partial T_f}{\partial t}\right) = \sum_{j=1} hc_j S_j\left(T_{j,pi} - T_f\right) + \dot{m}\, h_{fg}$$

(10)

- At the riser and downcomer level

$$m_f c_p\left(\frac{\partial T_f}{\partial t} + U\frac{T_f - T_{f-1}}{\Delta x}\right) = hcS\left(T_{pi} - T_f\right)$$

(11)

2.4.5 Heat transfer coefficients

The convective exchange coefficient between the external walls and the ambience can be calculated by [16,17]:

$$hc_e = 5.7 + 3.8 \times v \tag{12}$$

The natural convection heat exchange coefficient between the vertical internal walls and the air in the habitat enclosure is determined using the correlation of Churchill and Chu [18,19]:

$$Nu = 0.68 + 0.67 Ra^{1/4} \left\{ 1 + \left(\frac{0.492}{Pr} \right)^{9/16} \right\}^{-4/9} \quad ; \quad \text{with } Ra \leq 10^9 \tag{13}$$

The convective exchange coefficient between the internal air of the habitat and the horizontal walls is calculated by the correlation proposed by MacAdams [20,21]:

$$Nu = 0.27 Ra^{0.25} \tag{14}$$

The convective heat exchange coefficient between the refrigerant and the inner walls of the evaporator is calculated by [17,22]:

$$hc_{evap} = 0.00122 \left\{ \frac{c_{pl}^{0.45} \rho_l^{0.49} \lambda_l^{0.79}}{\sigma_f^{0.5} h_{fg}^{0.24} \mu_l^{0.29} \rho_v^{0.24}} \Delta T_s^{0.24} \Delta P_s^{0.75} \right\} \tag{15}$$

The natural convection transfer coefficient during condensation between the fluid and the inner walls of the condenser is calculated by [17,23]:

$$hc_{cd} = 0.943 \left\{ \frac{\rho_l g \lambda_l^3 h_{fg} (\rho_l - \rho_v)}{\mu_l L_{cd} (T_s - T_p)} \right\}^{1/4} \tag{16}$$

The radiation heat exchange coefficient between two parallel rectangular walls (i and j) of the same area is calculated by the relation (17) [17]:

$$hr_{i,j} = \frac{\sigma (T_i + T_j)(T_i^2 + T_j^2)}{\dfrac{1}{\varepsilon_i} + \dfrac{1}{\varepsilon_j} - 1} \tag{17}$$

The radiation heat exchange coefficient between two perpendicular walls with a common side is deduced from relation (18) [17]:

$$hr_{i,j} = \sigma \varepsilon_i F_{i,j} (T_i + T_j)(T_i^2 + T_j^2) \tag{18}$$

The sky temperature is calculated by the following expression [16,20]:

$$T_{sky} = 0,0552 (Ta)^{1,5} \tag{19}$$

2.5 Climatic Conditions

In this work we use the typical days of March of the region of Mamou (Guinea). These are very hot days of the year with an average minimum temperature of about 298 K and maximum of about 308 K. The maximum global solar flux is 1000 W/m². The hourly variations of the solar flux and the ambient temperature are obtained from the sinusoidal functions as shown on Fig. 3.
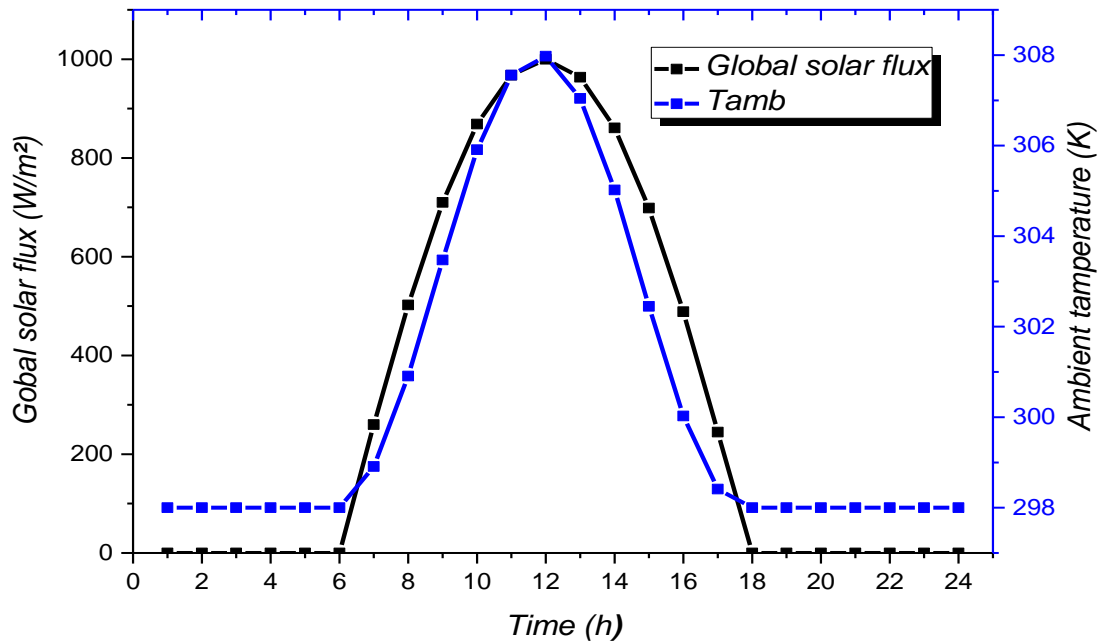
Fig. 3. Daily evolution of the horizontal global flux and the ambient temperature.

2.6 Method of Numerical Resolution

All heat transfer balance equations have been discretized and are solved by the implicit finite difference method based on the Gauss algorithm for the habitat and Thomas for the air conditioning system. It is an iterative calculation that determines the unknown variables at instant $t + \Delta t$ from the known ones at instant t.

3. RESULTS AND DISCUSSION

3.1 Evolution of the Solar Flux Density Incident on the Habitat

- On the roof

The slightly sloping, almost horizontal roof receives the highest solar flux and peaks at noon with a maximum value of 966.13 W/m². The solar flux incident on the roof is shown on Fig. 4.

- At the level of the vertical walls

The temporal evolution of the incident solar flux is linked to the orientation of each wall and also to the position of the sun at each moment of the day (sees Fig. 5). In this case, the most important flux arrives on the East wall with a peak at 10 am with a value of 671.93 W/m². This

flux decreases progressively until 1 p.m., which corresponds to the passage of the sun from the East to the West wall. From 1 p.m., the incident flux on the west wall increases to reach a peak at 3 p.m. with a value of 495.48 W/m² and it progressively decreases until it becomes zero at 6 p.m. In addition, the radiant flux on the south wall is greater than that on the north wall. The flux arriving on the South wall reaches a peak of 368.48 W/m² and 148.67 W/m² on the North wall at 12 h.

3.2 Model Validation

The numerical code of our model was validated by comparing our results with those obtained by Tong, Z & al [24] through an experimental study. They carried out an experiment on the self-regulation performance of thermosyphon loop with two evaporators installed in parallel. The working fluid is the refrigerant R744, unlike our system which works with the methanol. The temperature on the surface of the evaporator is measured with Pt1000 sensors. Fig. 6, shows a good qualitative agreement between our numerical simulation results and their experimental model. These results confirm the validity of the numerical code used for the simulation.
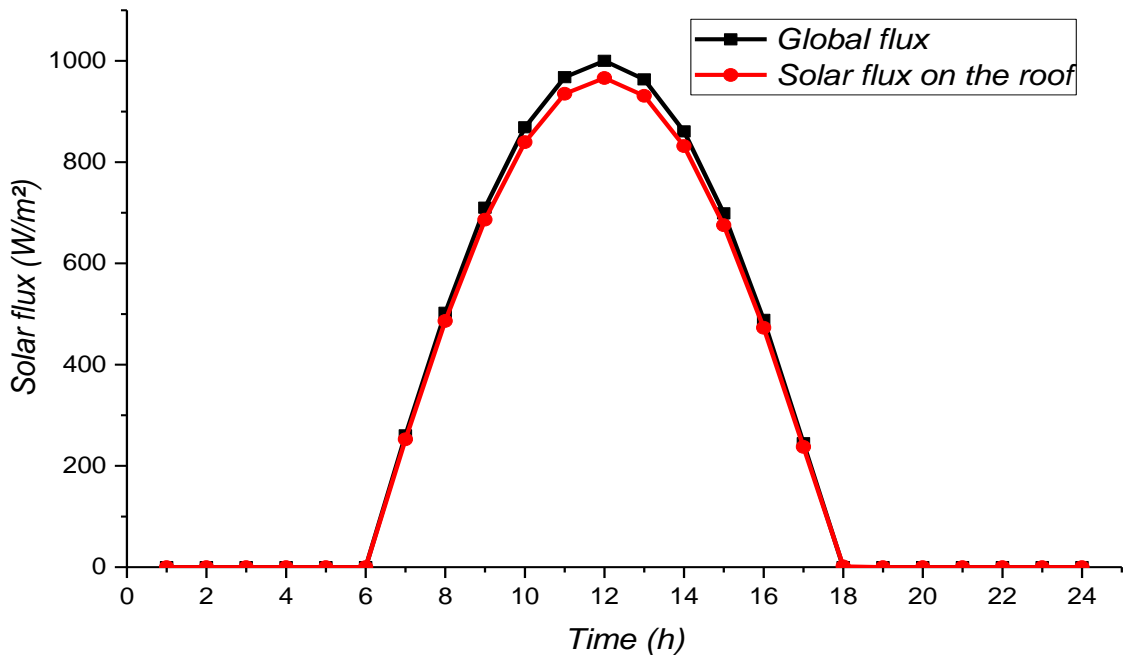
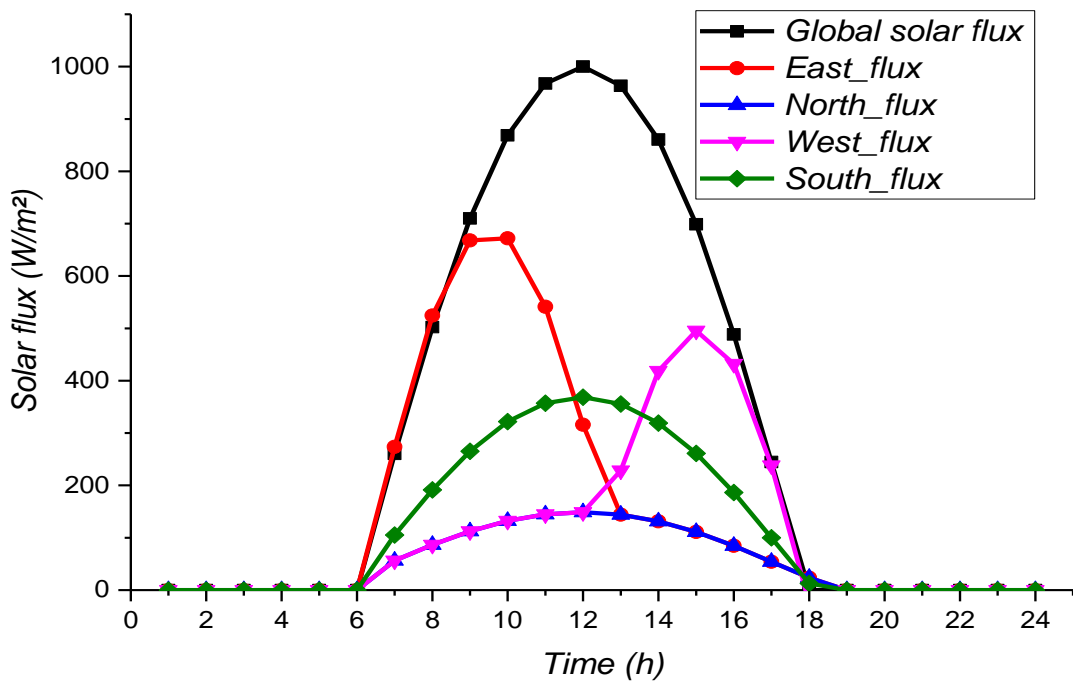**Fig. 4. Evolution of the solar flux density incident on the roof**

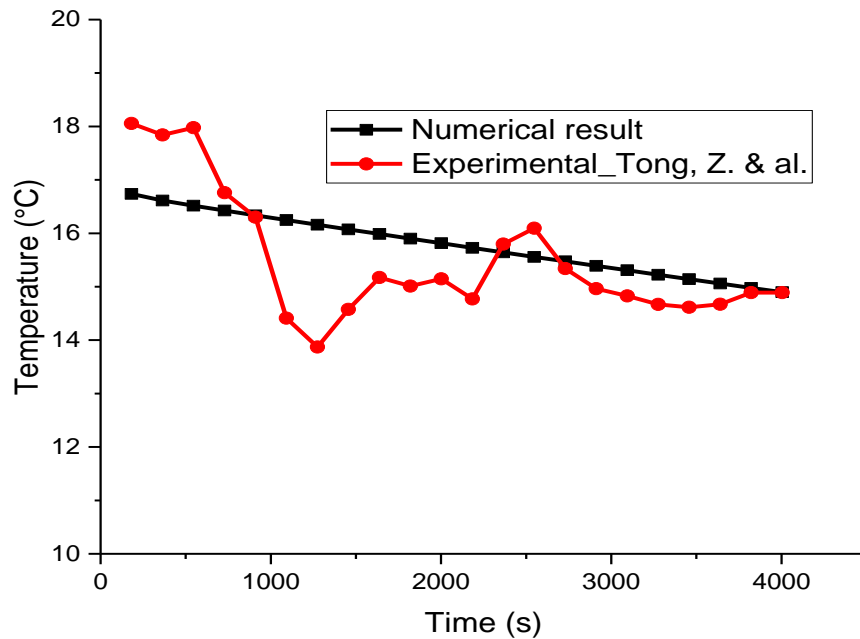**Fig. 5. Density of solar flux incident on the different vertical walls**

Fig. 6. Model validation from the evaporator

In addition we validated the numerical code of the habitat from the studies performed by Camara, Y. & al. [14]. They numerically studied a one-dimensional heat transfer in a habitable enclosure in hot countries. The results presented On Fig. 7, show the evolution of temperature profiles on the external roof of our habitat model and that of Camara Y. These results are in good qualitative agreement with an similar curves to the model studied. Indeed, differences in temperature are observed between our two models. This difference is mainly due to the fact that the thermo-physical properties of the materials are different. Our model uses galvanized steel sheets and clay bricks. On the other hand, Camara Y's study concerns a habitat with an aluminium roof and stabilized earth bricks.

3.3 Loop Temperature Profile

On Fig. 8, we show the temperature profile on the evaporator walls before and after coupling the habitat. A different curve shape was observed. The shape of the curve after coupling changes compared to the curve before coupling the habitat. This change is due to the variation of the ambient air temperature in the room to be cooled. This variation has an impact on the operation of the air conditioner. On the other hand, before coupling the ambient air temperature is constant. The maximum temperature value reached on the evaporator walls is about 287 K at 6 pm.

The temporal evolution of the temperature at the condenser is presented on Fig. 9. It is placed on the external East wall of the habitat with a surface of S=0.5 m². In the course of time, the temperature increases and reaches a peak of about 319.37 K at 14:00. This increase is mainly due to the release of heat during the condensation of the methanol vapour on the walls of the condenser and the physical phenomena of the environment (such as wind, solar flux, temperature, etc.).

The temporal evolution of the fluid flow rate at the condenser and evaporator is shown on Fig. 10. We are observing an important increase in fluid flow rate during the day and a tendency to decrease towards the evening. This is quite normal, as the operation of the air conditioner is ensured by a temperature difference between the medium to be cooled and the environment. An increase in this difference immediately leads to an increase in the flow rate in the loop. Thus, the maximum value of flow rate is about $2.71 \times 10^{-4}\ kg/s$ at the evaporator and $1.36 \times 10^{-4}\ kg/s$ at the condenser.
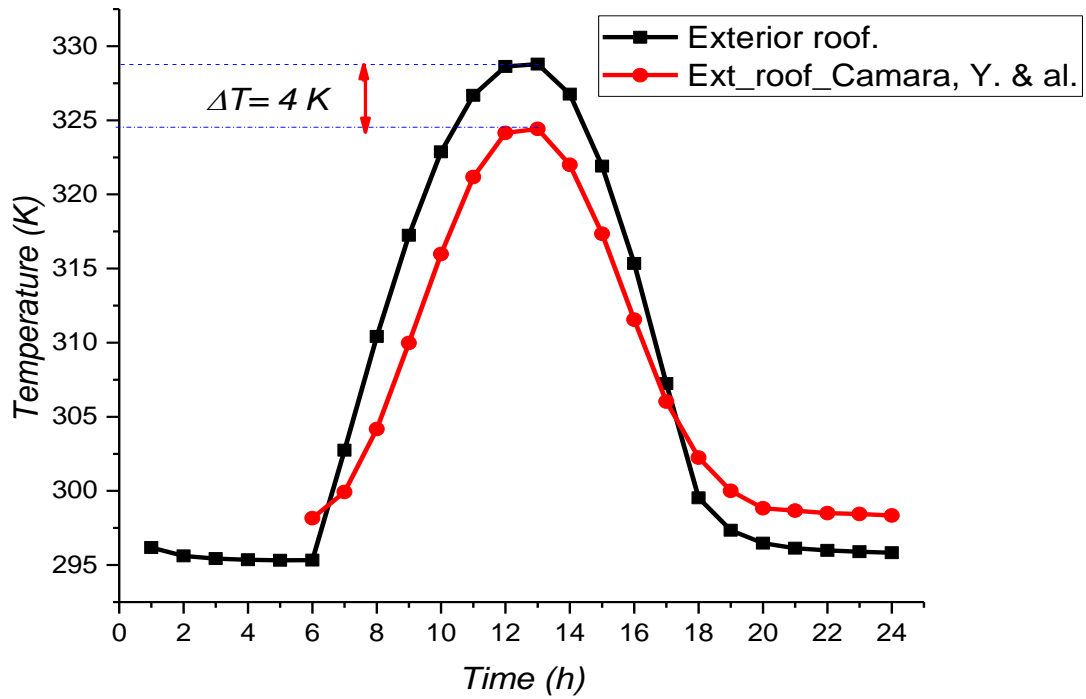
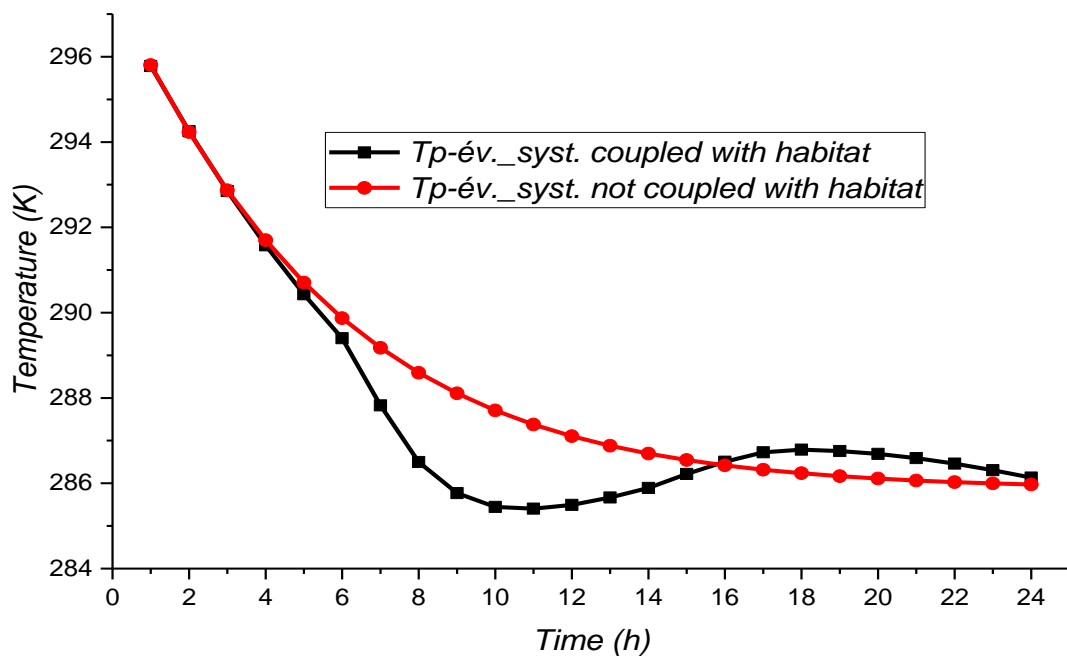**Fig. 7. Habitat model validation.**

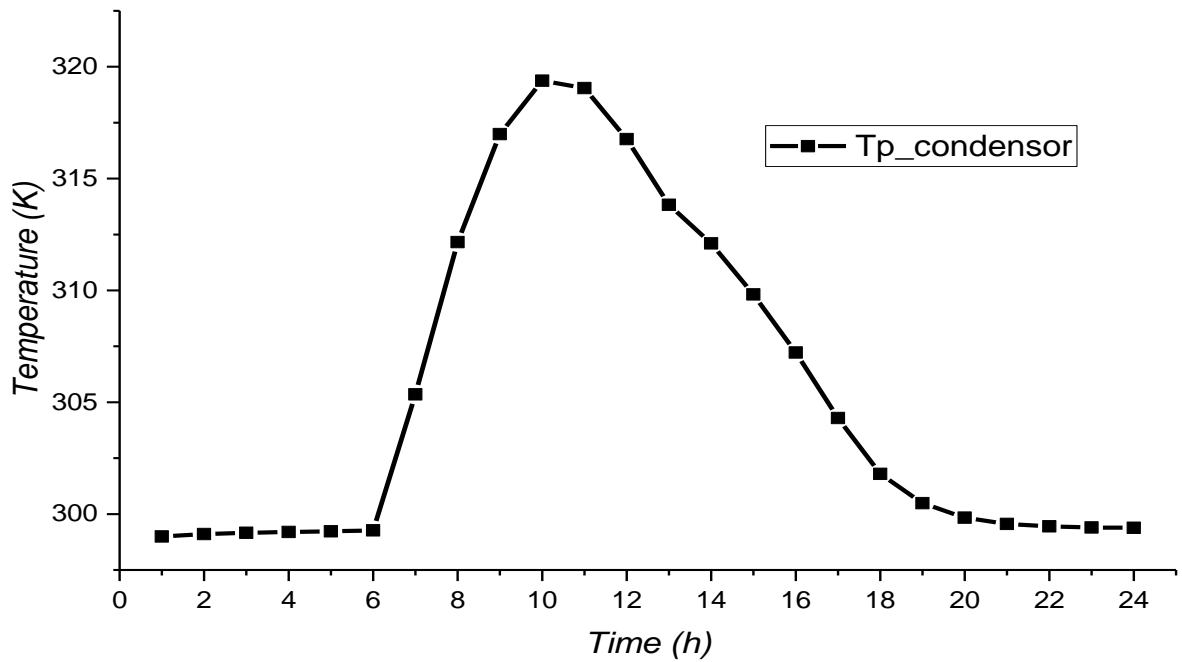**Fig. 8. Evaporator temperature profile before and after habitat coupling**

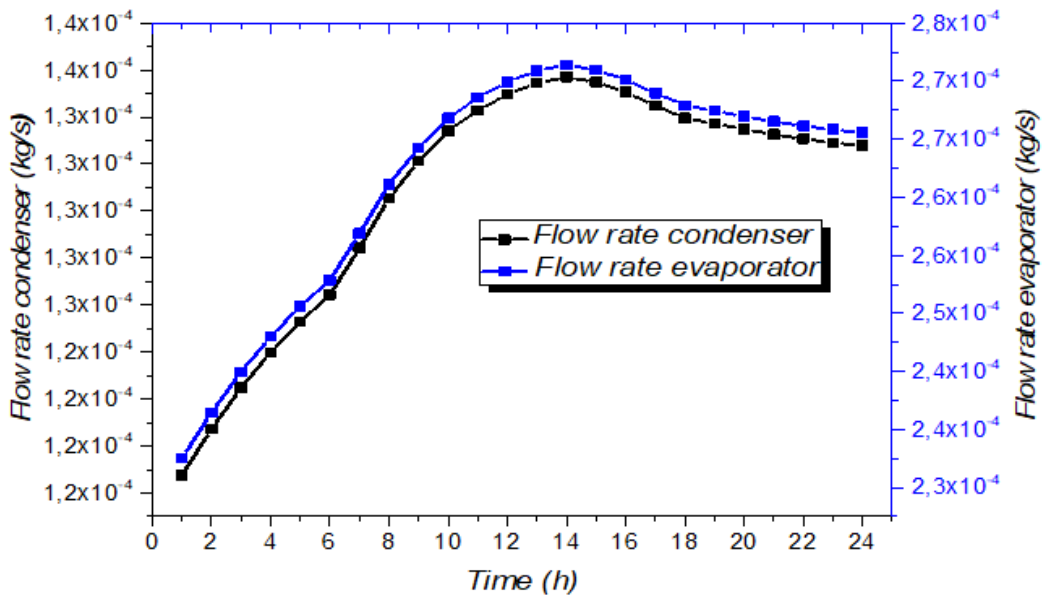**Fig. 9. Temperature evolution at the condenser**

Fig. 10. Evolution of the flow rate at the condenser and evaporator.

3.4 House Temperature Profiles with and without Air Conditioning

The Fig. 11. shows the evolution of the temperature profiles of the indoor air of the habitat before and after the coupling of the air conditioner. The numerical simulation was done with 15 cm wall thickness, an evaporator surface of 2 m² and without air exchange. The effect of the air-conditioning loop leads to the reduce the

temperature of the thermal environment. This decrease is due to the convective heat exchange between the air in the room to be cooled and the air in the evaporator. The heat from the room is captured by the evaporator by evaporating the refrigerant it contains towards the condenser. The maximum temperature of the air inside the habitat with the air conditioner is about 299 K à 15 h while the air temperature without the air conditioner is about 303 K at 3 p.m. The air conditioner has enabled to reduce the ambient temperature in the living space 4 K.

The evolution of the temperatures profiles on the internal walls of the room with and without the air conditioner is shown on Fig. 12 and Fig. 13. The following results show us the effect of the air conditioner on the temperature of each wall of the habitat. It decreases the temperatures on all the walls. On Fig. 12, we observe a peak of temperature at 5 p.m. whose maximum value of temperature on the East wall with the air conditioner is equal to approximately 302 K. On the other hand, the temperature value on this wall without air conditioner is equal to 303 K. Also, on the curves of Fig. 13, the maximum temperatures of the walls with the air conditioner

are observed at 14 h for the false ceiling, at 17 h for the floor whose values are respectively equal to approximately 306 K and 300 K. On the other hand, the temperature values for these same walls without the air conditioner are respectively 307.12 K for the false ceiling and 301 K for the floor.

3.5 Influence of the Parameters on the Habitat Interior Air Temperature

We present on Fig. 14, the effect of the thickness variation on the indoor air temperature of the habitat with the air conditioner. The variation of the thickness of the wall from 10 cm to 40 cm allowed us to observe its influence on the temperature profile of the air in the living space. We find that the temperature profiles evolve below the curve for a habitat without air conditioner. A small thickness increases the discomfort of the room. The maximum temperature values reached for a thickness of 10 cm, 15 cm or 40 cm are 301.5 K, 297 K and 296.9 K respectively. However, the temperature for a habitat without air conditioning is 303 K, when the wall thickness is 15 cm.
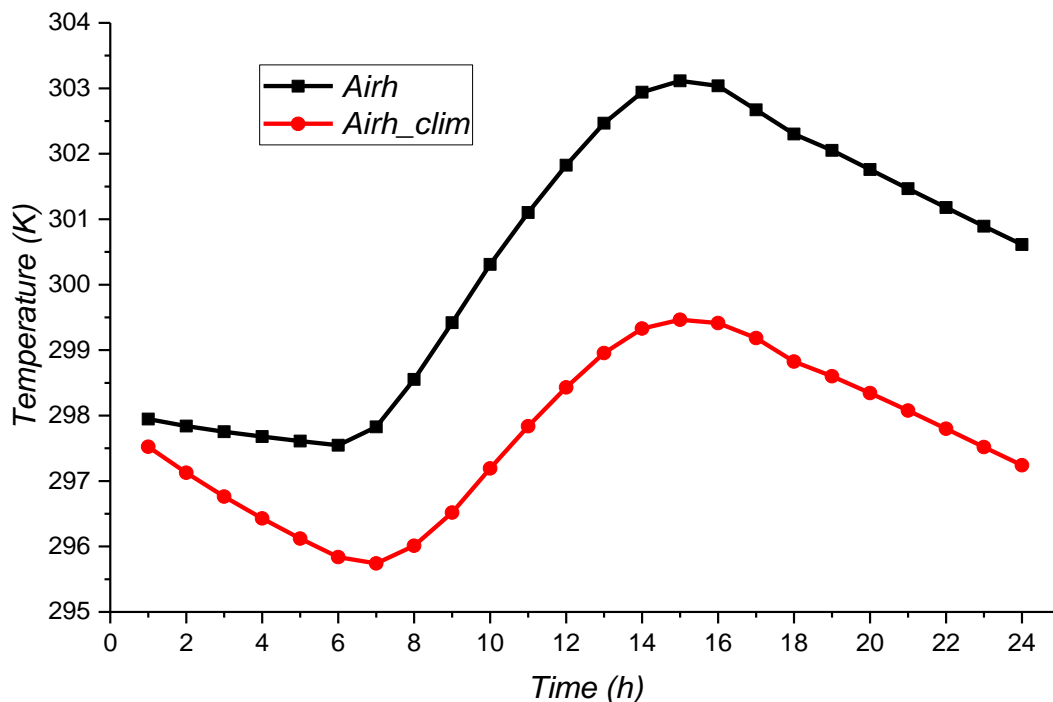

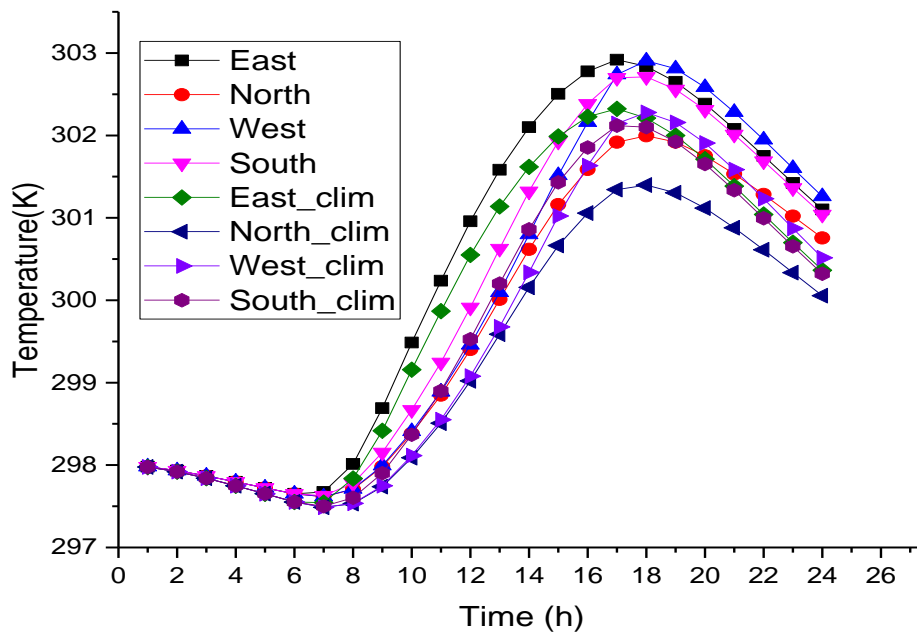**Fig. 11. Temperature profiles of indoor air with and without air conditioner**

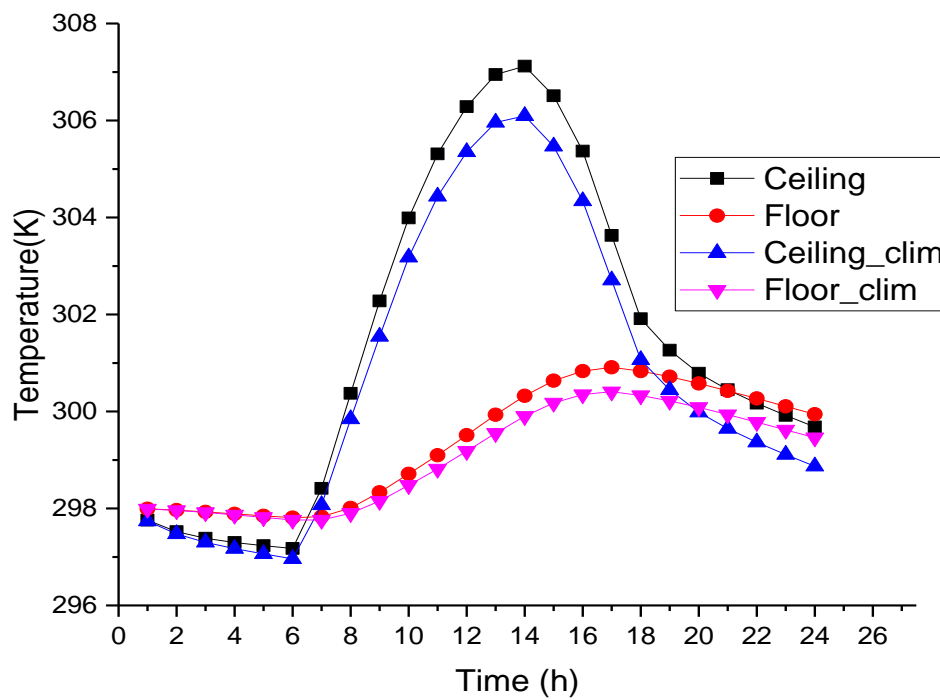**Fig. 12. Temperatures profile on the internal vertical walls of the room with and without the air conditioning loop**

Fig. 13. Temperatures profile on the internal vertical walls of the room with and without the air conditioning loop
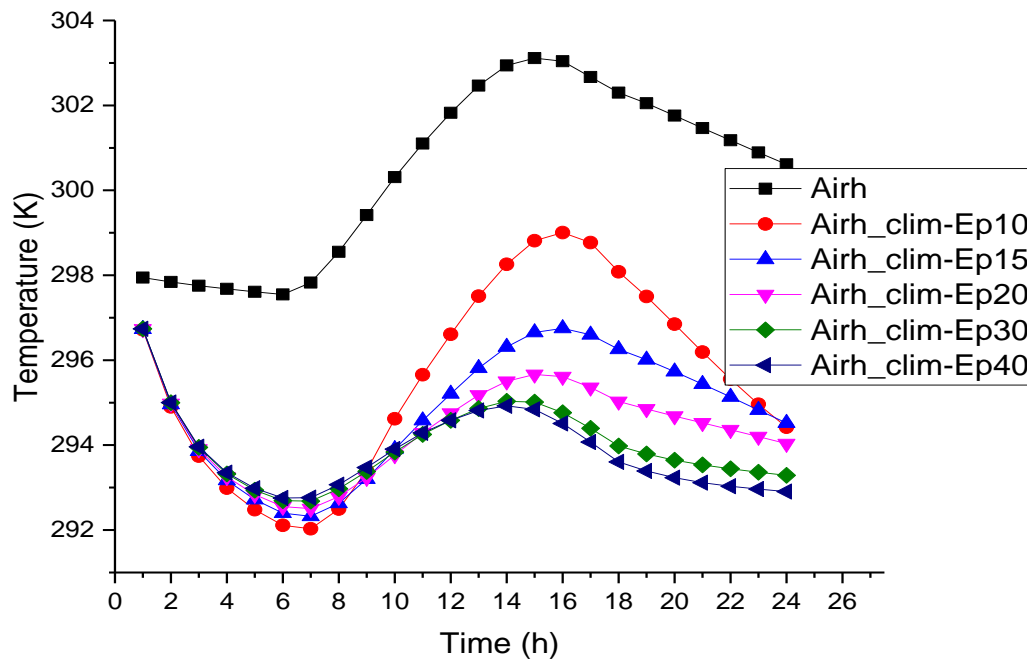
15

Fig. 14. Effect of wall thickness variation on the interior air temperature of the habitat with the air conditioner

The Fig. 15 also shows the effect of the variation of the air exchange rate on the air temperature profile of the room coupled to the air conditioning unit. Air infiltration through open doors or windows has a negative impact on the operation of the air-conditioning unit and thus leads to an increase of the air temperature in the room. At an air change rate of N=10, the maximum value of temperature of the room air is about 303.6 K at 2 p.m.

We have varied the intensity of the solar flux incident on the habitat from 900 W/m² to 1500 W/m² to observe the impact of this on the cooling of the room (Fig. 16). It is obvious that solar radiation has a very important effect on cooling. The increase of the solar flux also leads to the increase of the temperature of the air-conditioned room. We are observing on the curves that in the absence of the sun, the thermal load in the room is almost stable. For a maximum flux of 1500 W/m², the maximum value of temperature reached in the room is 301.5 K from 3 pm.

We varied the maximum ambient temperature from 308 K to 318 K (Fig. 17) and the minimum ambient temperature from 288 K to 303 K (Fig. 18) in order to observe the impact of these

temperatures on the temperature of the air inside the room equipped with the air conditioner. We note that these variations have an influence on the internal temperature of the room and also on the operation of the air conditioning unit. When the temperature of the room increases, the temperature difference between the room and the ambience decreases and the performance of the air conditioner decreases. This leads to an increase in the internal temperature.

The influence of the variation of the evaporator surface on the temperature of the air inside the room is shown on the Fig. 19. The simulation was carried out with a wall thickness of 15 cm, without air exchange and a maximum solar flux of 1000 W/m². We varied the surface of the evaporator from 0.5 m² to 3 m² to observe the impact of this surface on the cooling of the room. The results show that the larger the surface area, the greater the convective exchange between the air in the room and the evaporator walls, and decrease the temperature of the air inside the room. The maximum value of the temperature of the air inside the room is equal to approximately 298 K for an evaporator surface of 3 m² and approx. 302 K for a surface of 0.5 m².
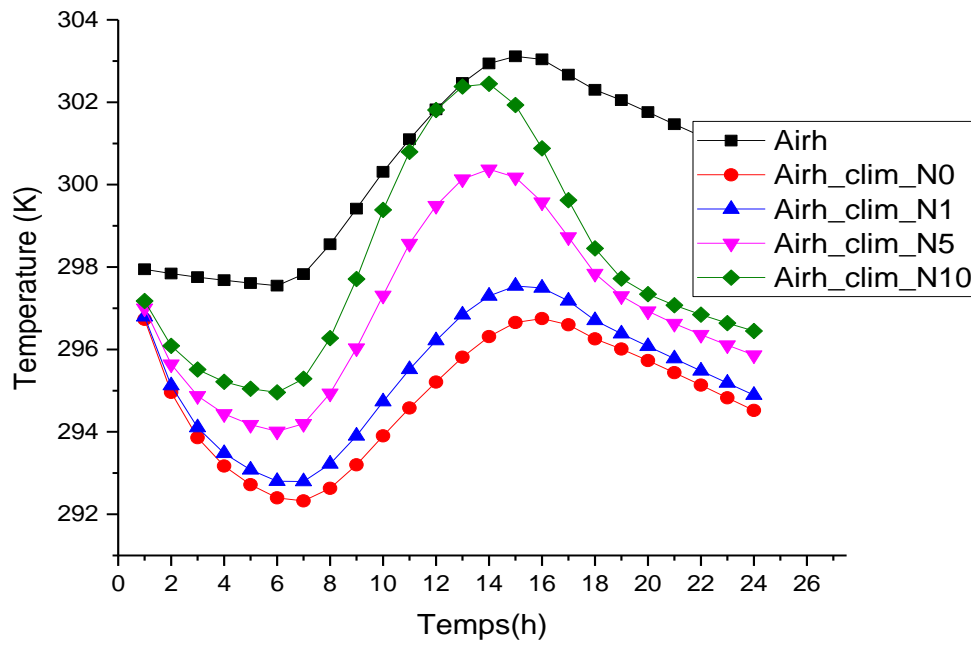
Fig. 15. Effect of the variation of the air exchange rate on the air temperature of the room equipped with the air conditioner
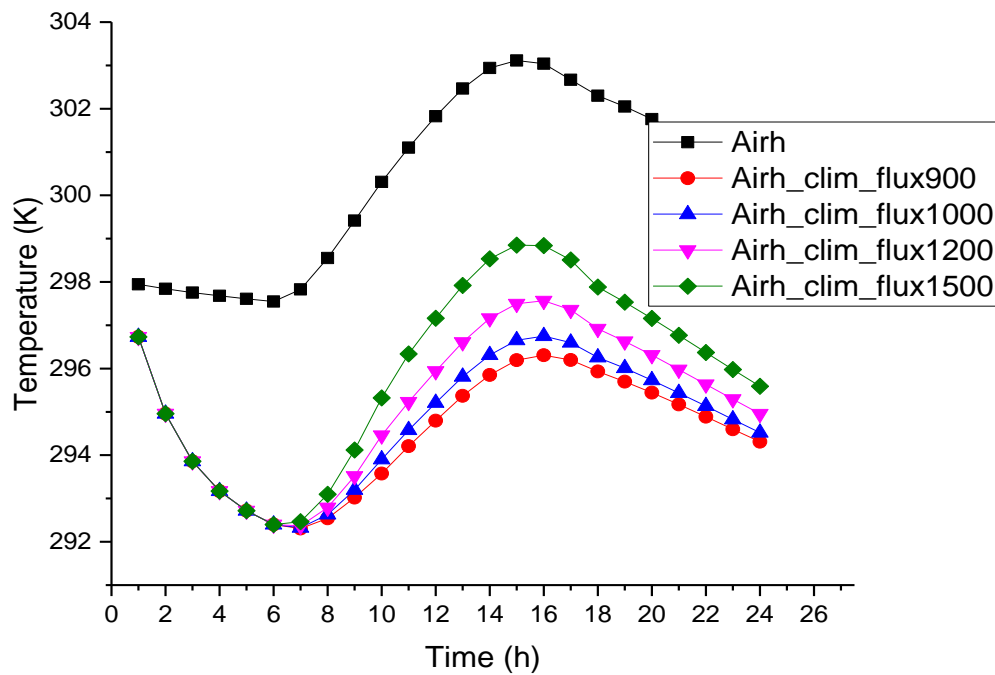

Fig. 16. Influence of the variation of the solar flux on the temperature of the air inside the room equipped with the air conditioner
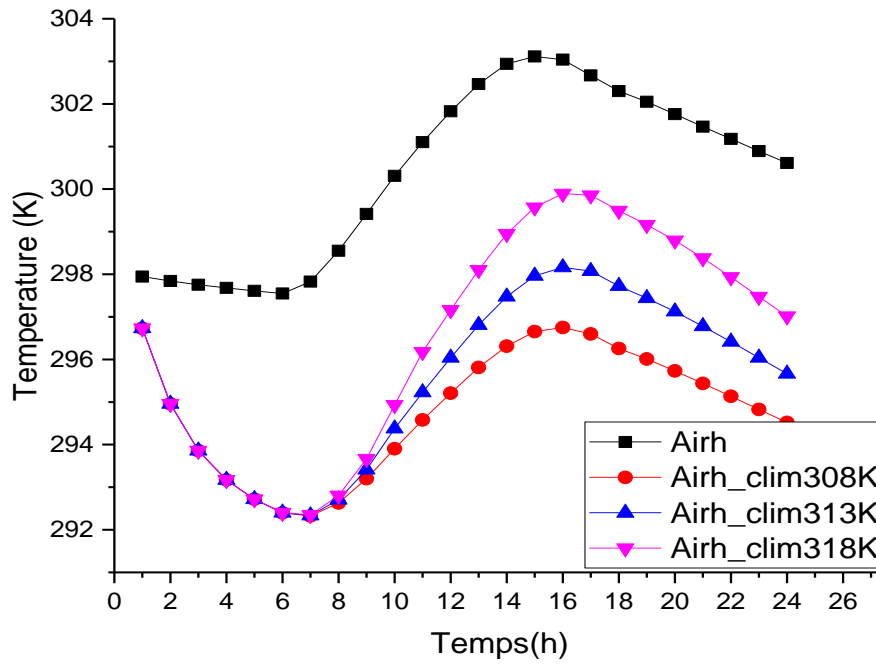
Fig. 17. Influence of the maximal temperature on the air temperature in the room equipped with the air conditioner
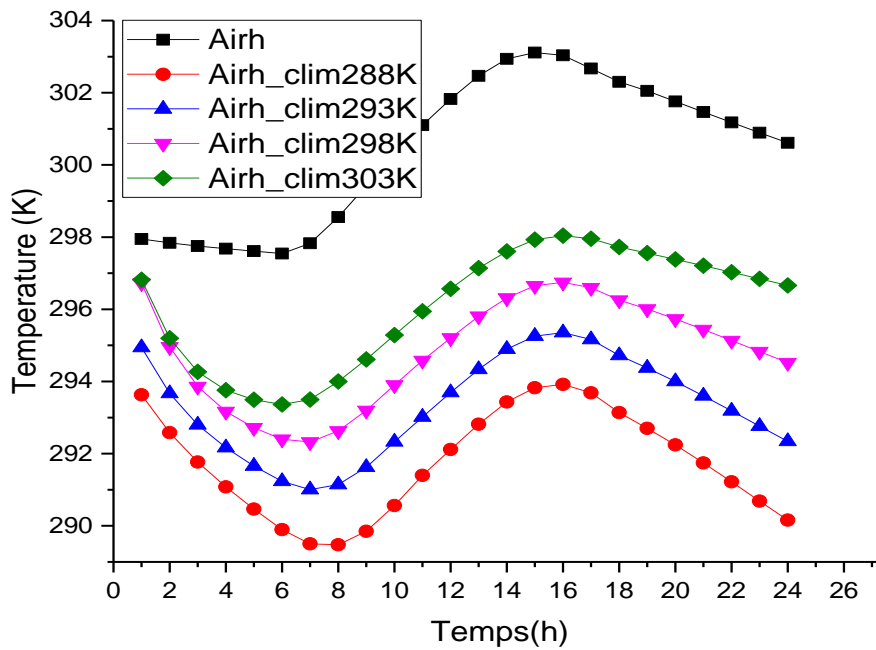

Fig. 18. Influence of the minimum temperature on the air temperature in the room equipped with the air conditioner
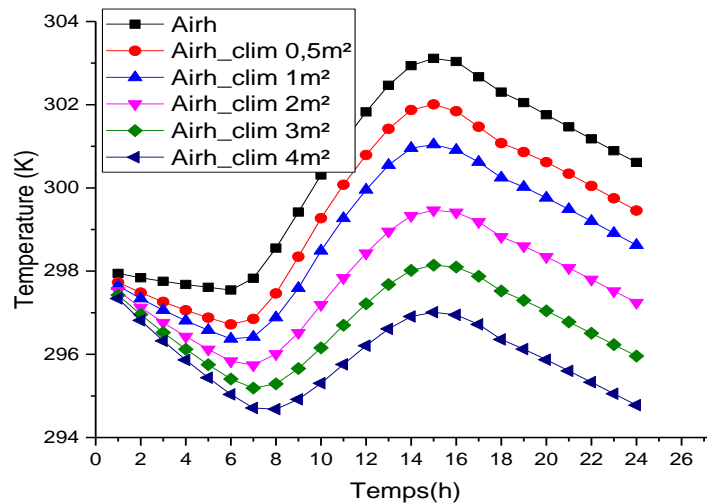
Fig. 19. Influence of the evaporator surface on the interior air temperature of the habitat.

4. CONCLUSION

In this paper, we have presented a numerical study of the passive air-conditioning of a room by a two-phase thermosiphon loop. The heat transfer equations were solved by the implicit finite difference method. A computational code written in Fortran was applied to the physical model using meteorological data for typical days in March in Mamou (Guinea). The results of a habitat with and without the air conditioning loop were also presented. They showed the feasibility of the air-conditioning loop in cooling the habitat by lowering the indoor air temperature. The value of the indoor air temperature reached is about 299 K, while that of the air in the living space without the air conditioner is equal to 303 K. The variation of the parameters (evaporator surface, wall thickness, temperatures, solar flux, air renewal) has a considerable impact on the cooling. Indeed, the larger the evaporator surface, the better the thermal comfort of the room. On the other hand, a low wall thickness or a high air exchange rate contributes to the temperature increase in the room. For a wall thickness of 10 cm, 15 cm or 40 cm, the air temperatures are 301.5 K, 297 K and 296.9 K respectively. However, for a habitat without an air conditioner the temperature is 303 K when the wall thickness is 15 cm. The right choice of these parameters will increase the thermal performance of the loop. This will provide acceptable comfort for the occupants.

COMPETING INTERESTS

Authors have declared that no competing interests exist.

REFERENCES

1. Bhamare DK, Rathod MK, Banerjee J. Passive cooling techniques for building and their applicability in different climatic zones—The state of art. Energy and Buildings. 2019;198:467-490.

2. Santamouris M, Sfakianaki A, Pavlou K. On the efficiency of night ventilation techniques applied to residential buildings. Energy and Buildings. 2010;42(8):1309-1313.

3. MEH, PNUD. Evaluation et Analyse des Gaps par rapport aux objectifs de SE4ALL, Rapport final 1; 2014. Avaialble:www.se4all-africa.org/fileadmin/uploads/se4all/Docume nts/Country_RAGAs/Guinea_RAGA_FR_R eleased.pdf

4. Ibrahim E, Shao L, Riffat SB. Performance of porous ceramic evaporators for building cooling application. Energy and Buildings. 2003;35(9):941-949.

5. Le Masson S, Mecheri B, Louahlia-Gualous, H, Nortershauser, D. Boucle diphasique à minicanaux pour le refroidissement de cartes de télécommunication. Sd.

6. Franco A, Filippeschi S. Experimental analysis of closed loop two phase

thermosyphon (CLTPT) for energy systems. Experimental thermal and fluid science. 2013;51:302-311.

7. Mecheri, B. Refroidissement d'une armoire de télécommunication avec bouche diphasique thermosyphon (Thèse de doctorat, Belfort-Montbéliard); 2011.

8. Chehade A, Louahlia-Gualous H, Le Masson S, Lépinasse E. Experimental investigations and modeling of a loop thermosyphon for cooling with zero electrical consumption. Applied Thermal Engineering. 2015;87:559-573.

9. Cao H, Ding T, He Z, Li Z. Recherche sur la hauteur de colonne de fluide frigorigène dans le déversoir d'un thermosiphon à boucle diphasique. Journal international de la refrigeration. 2018;94:40-48.

10. Zhang P, Wang B, Shi W, Han L, Li X. Modélisation et analyse des performances d'une boucle thermosiphon diphasique avec déversoir partiellement/entièrement rempli de liquide. Revue internationale du froid. 2015;58:172-185.

11. Khodabandeh R, Furberg R. Heat transfer, flow regime and instability of a nano-and micro-porous structure evaporator in a two-phase thermosyphon loop. International journal of thermal sciences. 2010;49(7):1183-1192.

12. Tong Z, Liu XH, Li Z, Jiang Y. Experimental study on the effect of fill ratio on an R744 two-phase thermosyphon loop. Applied Thermal Engineering. 2016;99:302-312.

13. Tong Z, Ding T, Li Z, Liu XH. An experimental investigation of an R744 two-phase thermosyphon loop used to cool a data center. Applied Thermal Engineering. 2015;90:362-365.

14. Camara Y, Chesneau X, Kante C. Etude numérique du confort thermique dans un habitat bioclimatique en brique de terre stabilisée pour un climat type de la Guinée. Afrique Science. 2018;14(2):238-254.

15. Kaboré, B, Wende Pouiré Ouedraogo G, Ousmane M, Zoma V, Zeghmati B, Chesneau X, Joseph Bathiébo, D. Habitat cooling by a canadian well in ouagadougou (Burkina Faso): Numerical approach. Physical Science International Journal. 2021;25(10):21-28.

16. Oudrane A, Aour B, Zeghmati B, Chesneau X, Hamouda M. Analyse numérique du transfert de chaleur unidimensionnel pour la maison du désert. Recueil de mécanique. 2017;2(01):089-102.

17. Diallo A, Chesneau X, Diaby I, El-Maktoume D. Modelling of a two-phase thermosyphon loop for passive air-conditioning of a house in hot and dry climate countries. Energy and Power Engineering. 2021;13(6):243-260.

18. Khalifa AJN. Natural convective heat transfer coefficient–a review: I. Isolated vertical and horizontal surfaces. Energy conversion and management. 2001;42(4):491-504.

19. Churchill SW, Chu H H. Correlating equations for laminar and turbulent free convection from a vertical plate. International journal of heat and mass transfer. 1975;18(11):1323-1329.

20. El-Maktoume D, Chesneau X, Diallo A, Randriamanantany ZA. Study of habitat's thermal performance equipped with an adsorption cooling unit by geothermal heat pump. Journal of Power and Energy Engineering. 2021;9:26-52.

21. Camara Y. Etude numérique des performances thermiques d'un habitat bioclimatique (Doctoral dissertation, Perpignan); 2018.

22. Salem MAM. Experimental study for transient response of a double-tube thermosyphon (DTTH); 2010.

23. Naresh Y, Balaji C. Thermal performance of an internally finned two phase closed thermosyphon with refrigerant R134a: A combined experimental and numerical study. International Journal of Thermal Sciences. 2018;126:281-293.

24. Tong Z, Liu XH, Jiang Y. Experimental study of the self-regulating performance of an R744 two-phase thermosyphon loop. Applied energy. 2017;186:1-12.

Peer-review history:
The peer review history for this paper can be accessed here:
https://www.sdiarticle5.com/review-history/82822